COMMONWEALTH OF AUSTRALIA

DEPARTMENT OF NATIONAL DEVELOPMENT

BUREAU OF MINERAL RESOURCES, GEOLOGY AND GEOPHYSICS

Record No. 1970/109

Design of Proton Magnetometer MNS 2
Preliminary Report

by

K. Seers

Record No. 1970/109

Design of Proton Magnetometer MNS 2
Preliminary Report

by

K. Seers

CONTENTS

1. HISTORY

In 1967 it was proposed that the Design and Development Group (now Instrument Development Group) of the BMR Geophysical Laboratories should develop a general purpose proton precession magnetometer (PPM) because of the lack at that time of any commercial unit which was generally suited to the various requirements imposed by airborne, marine, observatory, and portable ground station applications. The use of PPMs in all these fields was expected to increase, and rather than purchase several different commercial units which were expensive, not readily interchangeable and, in some cases, not adequate for the job, it was decided to use the Group's past experience in PPM design to incorporate into the one instrument all the features required by the potential users within BMR. The attainment of this aim in a portable instrument was made possible by the use of integrated circuits (ICs), which were becoming readily available at that time.

The original proposal was to duplicate the major features of a previously designed airborne PPM, the MNS1, add any additional features required, and replace discrete circuitry with ICs where possible. However, it soon became apparent that this approach, although workable, did not take full advantage of the versitility offered by ICs, so the MNS2 resembles the MNS1 only broadly in block diagram form. At the time of writing this preliminary report (August 1969) work is continuing on the development of the signal circuits (preamplifier and phase locked loop) to obtain optimum performance at the rapid cycling rates required in airborne applications. For other applications most design aims have been realised, and it is proposed to have three units built for general purpose work. The modular construction employed will enable these three units to be updated when final design is complete.

2. BLOCK DIAGRAM

The MNS2 simplified block diagram is shown in Figure 1. The principles of proton precession and the PPM are outlined in Appendixes A and B. Operation of the magnetometer is as follows. The polarising circuit receives a cycle pulse, in one of three ways: automatically after the previous operating cycle, manually from a front panel control, or from an external source. This pulse disconnects the detector from the preamplifier, resets the field counter and time base dividers, activates the frequency detector in the phase locked loop (PLL), and turns on the solid-state polarising switch to supply polarising current to the detector during a time interval set by an internal switch. At the conclusion of this time the polarising current is turned off (the stored magnetic energy in the detector being dissipated in a zener diode and resistor network), the reset signal is removed from the counter and time base, and the preamplifier is connected to the detector. The detector signal is only a few microvolts at about 2 kHz and decays with a time constant of about one second. To obtain a direct reading in nanotesla (nT)* with a resolution of 1 nT or better

---

* In line with international engineering practice the SI system of units is used in this report. The unit of magnetic induction, the

gamma, commonly used by geophysicists is not admissible in this system, the equivalent being the nanotesla which equals 10^{-9} tesla. It is the opinion of the author that in the interests of interdisciplinary communication the term gamma ought to be discarded completely.

---

in about 0.1 second, the precession signal frequency is multiplied by 200 in two stages. After filtering and amplification, the detection of both zero crossings gives a multiplication by two and a phase-locked oscillator provides further multiplication by 100. The PLL frequency detector ensures rapid acquisition of the signal, and a frequency difference detector, believed to be novel, was developed for this circuit. Because of the time required for the PLL to acquire the signal and settle to its steady state condition, a preset buffer time initiated at the depolarising instant delays the turning-on of the gating circuits. During the buffer time the frequency detector is turned off, allowing the phase detector to assume sole control of the PLL.

At the conclusion of the buffer time two gates are turned on. One allows the crystal oscillator signal to pass to the time base dividers; the other allows the voltage controlled oscillator (VCO) output to pass to the field counter. The duration of the counting time depends on the required resolution and is set by a front panel control. When this time has elapsed the time base output turns both gates off.

The frequency of the crystal oscillator, 85.1518 kHz, is chosen to give an absolute direct reading in nanotesla, and at the end of the counting time the count held by the field counter is read into a memory circuit where it is stored until the next count is completed. The memory circuit has binary coded decimal (BCD) outputs for each of its five decimal digits, and these outputs are available via a rear panel connector for use with data acquisition systems. The BCD memory outputs are also decoded to drive numerical indicator tubes and are fed to a digital-to-analogue converter for driving chart recorders. The pulse that sets the memory is also used to initiate the next cycle, if automatic cycling is selected.

The power supply is a regulated d.c. convertor providing five different output voltages including the 300 volts required by the numerical indicator tubes.

Several features of the prototype are not shown on the simplified block diagram. One of these is a variable preset delay, ranging from five seconds to a minute, which can be inserted in the cycle line. This would be used in ground station applications when automatic cycling is required, but frequent readings are unnecessary and in fact undesirable because of the considerable battery drain during polarising. In the interests of conserving batteries still further in such applications, a circuit is presently being considered which will turn the magnetometer off between readings. If this circuit is used it is expected that it could be adjusted for reading rates ranging from once per 30 seconds to once per 30 minutes.

Other features not shown include various self-checking facilities and the switching arrangements associated with tuning, resolution, and cycling.

3. PERFORMANCE AND OTHER CHARACTERISTICS

The performance characteristics outlined in the following sub-sections basically represent the original design aims. Subject to environmental tests, and with the exception of those characteristics that require cycling rates in excess of once per second, most have been achieved in the present prototype MNS2.

3.1 Tuning ranges

Ten switched ranges are provided, each having a bandpass of 10,000 nT, giving an effective coverage from 5000 nT to 105,000 nT. As yet no testing has been carried out to verify that usable signal is obtainable from fields as low as 5000 nT. However, as fields as low as this could be encountered in observatory vector measurements, the figure still stands as a design aim. In the prototype, only five consecutive tuning ranges are selectable by the first five positions of the function switch on the front panel. An internal patch plug selects the five ranges desired. In the final design the tuning switch may be separate to allow any range to be selected from the front panel.

A monitor lamp to indicate signal strength is an aid to tuning in an unknown field.

3.2 Resolution

The longer the multiplied precession frequency is counted, the greater the resolution. But, because the signal decays expenentially, a practical limit is placed on resolution by both the noise figure of the preamplifier and the PLL noise bandwidth. The polarising time and the type of detector determine the initial signal amplitude and the decay time constant, so these too can limit the resolution.

With a polarising time of five seconds, a resolution of 0.1 nT has been obtained from the prototype. Better resolution is probably obtainable but further testing is required.

A five-position front panel switch varies the counting time to give resolution of 0.1, 0.5, 1, 5, and 10 nT, the higher resolutions being realisable only for long polarising times. The counting time for 1 nT resolution is approximately 0.117 seconds.

3.3 Cycle times

Cycle time is the sum of the polarising time, buffer time, and counting time. The buffer time is fixed and the counting time is set by the resolution switch. An internal five-position switch selects the required polarising time. For a resolution of 1 nT the four available polarising times give nominal cycle times of 0.5, 1, 2,

and 5 seconds. In its fifth position, the switch inserts the cycle delay mentioned in the second to last paragraph of Chapter 2, the polarising time being the same as that for a nominal 5-second cycle.

Each polarising time is separately adjustable so that cycle times intermediate between those above may be chosen.

3.4 Figure of merit

The performance of a PPM is usually judged by the obtainable resolution and cycle time. In comparing different magnetometers the author has found it convenient to assign a simple figure of merit M, defined as the reciprocal of the product of the cycle time in seconds and the resolution in nT. In general, M is a function of resolution for a given magnetometer. The design aim for the MNS2 is $M \geq 2$ for resolutions of 1 nT to 0.1 nT, falling to M = 0.25 for a resolution of 10 nT. This compares with M = 0.67 at 1 nT resolution for the "Elsec" portable PPM.

3.5 Count scatter

In any digital counting system there is always the possibility of ambiguity of $\pm$ 1 in the count. In addition to this source of scatter, random noise superimposed on the signal will also contribute to count scatter. It is hoped to be able to achieve a counting standard deviation equal to or less than the nominal resolution; i.e. for a resolution of 1 nT, 68 percent of all counts should be within $\pm$ 1 nT of true value. This has been achieved for slow cycling.

3.6 Absolute accuracy

Absolute accuracy depends only on the accuracy and stability of the crystal oscillator. No tests have been carried out as yet, but it is predicted that absolute accuracy will be maintained to better than 1 part in 10^5.

3.7 Cycline modes

A three-position lever switch on the front panel controls the cycling. In the centre position, cycling is from any one of three external sources: (i) an IC compatible pulse applied via the digital output or power connector on the rear panel; (ii) an earthing contact closure applied via the power connector; (iii) an earthing contact closure applied via the detector connector on the front panel. It is envisaged that this last method of cycling would be used in portable applications, where the operator could cycle the unit from a switch on the detector staff, leaving the other hand free to record the reading.

In the "up" position cycling is automatic, the end of one cycle initiating the start of the next.

The "down" position is spring loaded to return to centre, and this is used to cycle manually from the front panel.

When switched in, the cycle delay operates on all the above cycling modes, as does a cycle-inhibiting feature which prevents the magnetometer from being cycled while it is counting. Without this feature a premature cycling command would interrupt or reset the previous count before it was stored in the memory.

Should the magnetometer be required to cycle associated equipment, a pulse corresponding to the polarising time is available at the digital output connector.

3.8 Readout

The field counter consists of five decades. This means that for resolutions of 0.5 and 0.1 nT the most significant digit is lost, but, as it can be determined by switching to a lower resolution, the addition of a sixth counting decade and associated readout circuits was considered unnecessary. In any case, the most significant digit is seldom required even for lower resolutions.

As well as the numerical indicator display on the front panel there are two other forms of readout available on the rear panel. One is a parallel BCD digitial output for all digits, with low level true. The other is for driving strip chart recorders or other analogue devices. Each digit has an identical digital-to-analogue converter circuit, the outputs of which are selected by internal switches to drive the two recorder amplifiers. Each of these amplifiers has two summed inputs termed "units" and "tens". As the "tens" input is ten times as sensitive as the "units" input, the outputs of two consecutive digital-to-analogue converters may be summed to give 100 steps across the recorder chart. If desired the "units" input may be switched out so that only one digit is displayed by 10 steps across the chart. The switching is so arranged that any digit may be applied to the "tens" input of either (or both) amplifiers, while any digit other than the most significant may be applied to the "units" input of either (or both) amplifiers.

Each recorder amplifier has two outputs; one is for driving high-resistance recorders (5 volts full scale into 10 kilohms or higher), the other for driving galvanometer-type recorders such as the Esterline-Angus and Rustrak. The current available from the second output depends on the recorder resistance. Typical values are 4.5 mA into 100 ohms (or lower) and 1 mA into 4 kilohms (or lower). Both outputs may be used simultaneously. There are separate calibration adjustments for each output and a zero adjustment. Once these adjustments have been set the overall digital-to-analogue conversion error at the recorder input is less than 0.2 percent of reading.

A remote earthing contact applied via the power connector earths the recorder amplifier inputs so that recorder zeroing can be checked without disturbing the magnetometer.

3.9 Checking facilities

On position 6 of the function switch a constant signal derived from the crystal oscillator and having a frequency corresponding exactly to 50,000 nT is applied to the zero-crossing detector instead of the precession signal. A readout of 50,000 indicates that the PLL and gating circuits are operating correctly.

Positions 7 to 11 of the function switch are used to check the readout circuits. In position 7, pulses at about one per second are applied to the field counter and memory circuits. This enables the counting and readout for the least significant digit to be checked in about 10 seconds. In subsequent switch positions the frequency of the counter pulses is increased in decade steps so that all digits, recorder deflections etc. may be easily checked. Magnetometer cycling is inhibited in these switch positions and the monitor lamp, normally used to indicate signal strength, indicates the presence of the various internally generated power supply voltages.

3.10 Power supply

The unit is designed to operate from a (25 $\pm$ 3)-volt d.c. supply with negative ground. Quiescent current drain is about 1.8 amps. The polarising line has been kept separate from the main power line to reduce interference, but would normally connect to the same power source. There is no reason why a different polarising voltage should not be used, provided that the polarising current does not exceed 5 amps. Polarising current in amps is approximately one-eighth of the polarising voltage for the normal BMR detector.

Both lines are protected by fuses, but these will probably be replaced by minature circuit breakers. The power supply switching is so arranged that the power will not be connected if the polarity is incorrect.

3.11 Environmental performance

No testing under various environmental conditions has been carried out as yet, but all circuits have been designed to operate over an ambient temperature range of -10 to +60 °C. The design aim for vibration is that no damage shall result from vibrations in any plane, where the vibrations involve accelerations of 3g at any frequency up to 100 Hz. However, it would be expected that operation under these conditions would increase the count scatter considerably.

3.12 Construction

For high reliability, components meeting MIL or DEF specifications have been used where possible. Precautions will be taken to protect circuit modules and chassis materials from ill effects of operation in tropical, frigid, or arid zones.

Printed circuits are used wherever possible, to increase reliability and to reduce cost.

3.13 Dimensions

Height:	approximately 13 centimetres
Width:	approximately 22 centimetres
Length:	not yet finalised, but probably about 30 centimetres.

3.14 Adaptation to future developments

In airborne applications, noise in the towing cable may turn out to be the limiting factor for low count scatter. In this event the preamplifier and possibly the polarising circuits would have to be installed down-cable. The MNS2 has been designed to accommodate such a facility with no internal modifications or adjustments. The same detector connector would be used.

For very rapid cycling (more than twice per second) it may be possible to use a phenomenon observed in BMR magnetometers in 1962 and also reported by others, viz. the fact that a large signal can be built up by suitable phasing of the polarising with the precession signal. Space is to be left for one module card to provide phased polarising if it can be satisfactorily achieved. One or two extra front panel controls may be required, but no extensive modifications should be necessary.

4. SUMMARY OF WORK REMAINING

Although the prototype has given satisfactory results for most applications, the following work is still to be carried out to achieve the original design aims:

(1) Reduction of noise in preamplifier.

(2) Optimisation of PLL for both rapid acquisition and low noise band width.

(3) Testing of crystal oscillator stability.

(4) Testing at low field intensities.

(5) Environmental testing.

(6) Rationalisation of physical construction to combine ease of operation and maintenance with small size.

In addition, consideration will also be given to the incorporation of the slow cycle timer discussed in the second to last paragraph of Chapter 2, and at a later date, the inclusion of the phased polarising facility. Preliminary development of down-cable electronics has proved the concept to be feasible, but further work has been postponed until a need is demonstrated.

Determination of maximum obtainable resolution requires further testing.

5. CONCLUSION

The prototype MNS2 already combines most features found in a number of special purpose proton magnetometers; the only exception is cycling rates faster than once per second with a resolution of 1 nT. It is believed that very little further development is required to achieve this performance. Should this be so, the MNS2 will be the most versatile proton magnetometer yet produced (so far as is known), and the cost is estimated to be less than that for other special-purpose instruments.

When development and testing are completed a final report containing full details of circuit design, performance, and cost will be written.

APPENDIX A

THEORY OF PROTON PRECESSION

Both this and the following Appendix are intended for the general reader. A brief bibliography at the end of Appendix B suggests material for the reader who requires a more rigourous treatment.

The nucleus of the hydrogen atom, i.e. the proton, possesses the following two important properties:

(1) Spin angular momentum

(2) Magnetic dipole moment,

and may therefore be regarded as a tiny bar magnet spinning about its magnetic axis as shown in Figure A-1. In (a) the spin axis and the magnetic axis are said to be parallel while in (b) they are anti-parallel.

In a sample of hydrogen-rich liquid, such as water, kerosene, or oil, the protons are relatively free to orient themselves in the direction of any external magnetic field. Being thus aligned they would remain in this state were it not for the effects of thermal agitation.

At temperatures above absolute zero, heat energy is stored in the sample in the form of random motion of the atoms and molecules that comprise the sample; the higher the temperature, the greater the magnitude of random motion. It can be shown that one component of the random motion will act on the protons in such a way as to produce rotation in random directions. This is the thermal agitation referred to above.

Consider one proton which has been dis-oriented from the external field direction by thermal agitation. The spinning proton will be subjected to a torque that tends to rotate it back to its original orientation. Classical mechanics show that when a free-spinning system is acted upon by an external torque in the presence of retarding forces it will eventually align itself with the external force but in so doing will rotate bodily about the direction of the external force.

Note that in Figure A-2 the direction of rotation would reverse if either the spin direction or the external field direction were reversed, but not if both were reversed.

The rotation of a spinning body under the influence of an external torque is termed precession. It can be shown that the precession frequency, i.e. the number of rotations per second, is directly proportional to the magnitude of the external force. In the case of a proton in a magnetic field B,

$$2\pi f = \gamma_p B \qquad (1)$$

when f is the precession frequency in Hertz, γ_p is the gyromagnetic ratio for the proton and is a constant equal to 2.67519×10^8 rad sec $^{-1}$ tesla $^{-1}$, and B is the magnetic induction in tesla.

$$\therefore \quad f = 4.25770 \times 10^7 \, B \quad \text{Hz} \qquad (2)$$

The external field can therefore be measured by measuring f.

If the external field is the Earth's field (approx. 50,000 nT) the precession frequency will be about 2 kHz. Thermal agitation in the liquid sample will cause precession of individual protons, but because of the random phase of these individual precessions, no overall precession can be detected.

The function of the proton precession magnetometer is to provide:

(1) A means of obtaining coherent (in-phase) precession of the protons in the sample.

(2) A means of detecting this precession and measuring its frequency.

APPENDIX B

THE PROTON PRECESSION MAGNETOMETER

Consider a cylindrical sample of hydrogen-rich liquid situated inside a coil as shown in Figure B-1.

If a relatively large current I_p is passed through the coil from a d.c. source, a strong magnetic field B_p is produced inside the sample in its axial direction. If B_p is very much greater than the external field B_o, the effect of B_o can be neglected for the moment. In Appendix A it was pointed out that protons can exist in either the parallel or anti-parallel state. Quantum mechanics shows the parallel state to have the lower energy; hence we would expect to find more protons in this state. The ratio of populations of protons in the parallel and anti-parallel states is

$$\frac{\text{number parallel}}{\text{number anti-parallel}} = \exp\ (2\mu B_p/kT) \qquad (3)^*$$

where μ is the magnetic moment of the proton and is equal to 1.41049×10^{-26} joule tesla $^{-1}$.

B_p is applied magnetic field in tesla

k is Boltzmann's constant equal to 1.38054×10^{-23} joule $^{o}K^{-1}$

T is absolute temperature in ^{o}K ($0\ ^{o}K = -273.16^{o}C$).

The application of I_p tends to align the proton magnetic moments in the direction of B_p. This alignment is resisted by thermal forces, and an equilibrium is reached when the total number of protons aligned is directly proportional to B_p and inversely proportional to absolute temperature. The alignment of the protons does not occur instantaneously. Equilibrium is reached exponentially with time constant T_1, the spin-lattice relaxation time. For water, $T_1 = 2.3$ seconds, for kerosene 0.7 seconds. The process of aligning the protons in the direction of B_p is called polarising the sample. I_p is the polarising current and B_p, the polarising field, is typically 20 to 50 milliteslas.

If the polarising field is now removed very quickly (i.e. the sample is depolarised) so as to leave the protons momentarily aligned, they will all start to precess in phase about the direction of B_o. Because all protons are precessing in phase, their individual contributions can be added to produce a resultant rotating magnetic field inside the coil. A sinusoidal emf will therefore be induced in the coil. Emfs from protons in parallel and anti-parallel states add,

---

* This result is stated for general interest. It has no direct bearing on the operation of the magnetometer.

even though the directions of precession are opposite. A large polarising field is desirable for a large induced emf.

Precession cannot continue indefinitely as retarding forces caused by interaction between neighbouring atomic particles allow the proton to align itself eventually with B_o. The amplitude of the induced emf decays exponentially with time constant T_2, the spin-spin relaxation time. T_2 is always less than T_1.

The apparent decay time constant T_2' is often considerably smaller than the theoretical value for the following reasons:

(1) When the coil is connected to an external circuit (amplifier) the induced emf produces some in-phase component of current flow, and power is therefore dissipated. The energy to provide this power must be extracted from the magnetic energy of the precessing protons; i.e. the external circuit imposes a retarding force. This effect is known as radiation damping.

(2) If B_o is not completely uniform over the liquid sample but varies slightly from point to point, the precession frequency will also differ slightly from point to point. The resultant phase incoherence produces a retarding force. Field gradients as low as 20 nT per cm can render the signal useless. For this reason the sample should never be located near ferromagnetic materials when the magnetometer is operating.

It is obvious that precession cannot occur when B_o is in the same direction as B_p. If the angle between B_o and B_p is θ, it can be shown that the initial magnitude of the signal is proportional to $\sin^2 \theta$, i.e. is maximum for $\theta = 90^\circ$. Note that only the amplitude and not the frequency of the signal is a function of θ. For this reason the proton magnetometer measures total field magnitude and is not direction sensitive (apart from becoming insensitive as θ approaches 0°).

The open-circuit voltage V_{so} induced in the coil is given as a function of time t by the expression:

$$V_{so} = A\chi B_p \left(1 - \exp\left(-t_p/T_1\right)\right) \gamma_p B_o \sin^2 \theta \exp\left(-t/T_2'\right) \sin\left(\gamma_p B_o t\right) \qquad (4)$$

where A is a constant related to coil geometry;

χ is the nuclear paramagnetic volume susceptibility of the proton and is inversely proportional to absolute temperature. ($\chi = 3.3 \times 10^{-9}$ joule-tesla $^{-2}$ for protons in water at 300°K);

t_p is polarising time in seconds; and other symbols are as previously defined.

It is apparent that V_{so} is a damped sinusoid of initial amplitude $A\chi B_p (1 - \exp(-t_p/T_1)) \gamma_p B_o \sin^2\theta$, with frequency $\gamma_p B_o/2\pi = f_o$ Hertz, and damping constant $1/T_2'$.

For any practical coil, B_p is a complicated function of coil geometry and available polarising voltage. However, this effect may be absorbed into the constant A, and the value of B_p used is that which would occur in an ideal solenoid. A typical value for V_{so} for short polarising times would be 0.5 microvolts.

The low signal voltages available from the coil must be amplified before the frequency can be measured. The accuracy of this measurement depends largely on the signal-to-noise ratio at the amplifier output. There are four main sources of unwanted noise signals:

(1) Amplifier noise, which in a well-designed amplifier is mostly the noise contribution of the first stage.

(2) Detector noise which is caused by random motions of thermally energised conduction electrons. The noise voltage is given by

$$V_{nd} = \sqrt{4\ k\ TRB} \text{ volts} \qquad (5)$$

where k is Boltzmann's constant;

T is absolute temperature in ^{o}K

R is resistance of detector coil and connecting cable in ohms;

B is the bandwidth of the system in Hz.

Thus if $T = 300^{o}K$, $R = 10$ ohms, and $B = 500$ Hz, then $V_{nd} \simeq 9 \times 10^{-9}$ volts = 9 nanovolts. Detector noise is usually insignificant compared with amplifier noise.

(3) Noise pick-up from external sources. This can usually be reduced sufficiently by means of an electrostatic shield around the detector and the use of a balanced connecting cable. The low-level section of the amplifier should also be shielded.

(4) Microphonic noise due to amplifier vibration or motion of the detector cable. The former can be eliminated by shock mounting, the latter by the use of specially treated non-microphonic cables, although even these exhibit some noise.

It was previously pointed out that depolarising must be achieved very rapidly. The reason for this may be qualitatively explained as follows. Consider a proton aligned under the action of a polarising field B_p. The actual direction of the proton axis will be along the resultant field of B_p and the external field B_o. The direction of this resultant field will be almost exactly that of B_p if B_p is much greater than B_o. This is shown in Figure B-2 (a).

As B_p is reduced, the resultant field B_r does not initially change its direction very rapidly, but as B_p approaches equality with B_o, B_r changes direction more rapidly. It can be shown that when the time taken for B_r to change its direction appreciably is comparable with the precession period, precession will occur about a direction at right-angles to B_r, rather than about B_o. This destroys the $\sin^2\theta$ amplitude relationship, and the initial signal amplitude is no longer symmetrical about $\theta = 90^\circ$, nor is it maximum for $\theta = 90^\circ$. To avoid this effect it is desirable to remove the last few millitesla of B_p in a time much less than the precession period.

When the polarising current is turned off to remove B_p, the inductive nature of the coil gives rise to two undesirable effects:

(1) A back emf proportional to inductance and rate of change of current. This emf may be many thousands of volts, and unless limited in some way will cause permanent damage to wiring etc.

(2) Damped oscillations caused by resonance of the coil with its self-capacitance. The effect of these oscillations depends on their frequency and phase in relation to the phase of the precessing protons. In general they reduce the signal amplitude and produce an asymmetry in the $\sin^2\theta$ relationship.

To avoid the effects outlined above, the following requirements should be satisfied:

(a) The self-resonant frequency of the detector should be no less than about 10 kHz.

(b) The polarising current should be turned off so that the final part of B_p collapses in a few microseconds.

(c) The reverse voltage should be limited to 200 volts or less.

(d) A resistor should be connected across the coil to provide critical damping (i.e. no overshoot or ringing) during the final part of the decay.

Requirement (b) may be satisfied by using either a relay or a fast semiconductor switch. If a relay is used it must have no contact bounce when it breaks, and should be of the vacuum or mercury-wetted type to avoid the effects of contact arcing. Requirement (c) may be satisfied by connecting a voltage-dependent resistor or a zener diode across the coil.

The total time for depolarising is dependent on the actual circuit constants but is usually a few milliseconds.

Some amplifiers must be disconnected from the coil during the polarising and depolarising times to avoid damage by d.c. currents and switching transients. This may be achieved by means of relay contacts which should be gold-plated for use at low signal levels.

After all switching transients have passed, the frequency of the amplifier output is measured to obtain the value of the Earth's magnetic field. This measurement must be made very precisely. The Earth's field varies from about 40,000 nT at the equator to 70,000 nT near the poles. Local anomalies, caused by mineral deposits, may exceed 100,000 nT.

In geomagnetic surveying a resolution of one nanotesla is often required, i.e. a measurement of precession frequency with an error less than 1 part in about 50,000.

BMR has designed magnetometers in which one of two methods of performing this measurement is used, depending on the application:

Method 1: Used when measurements are not required in rapid succession and where a readout which is not directly in gammas can be tolerated. In this method, a known number of cycles n_p of the precession signal is used to gate the output of a 100-kHz crystal oscillator into a counter. If the counter registers n_c counts, the field is given by

$$B_o = \frac{n_p \times 10^7}{n_c \times 4.25759} \text{ nT} \qquad (6)^*$$

Note that B_o varies inversely as the counter output n_c and that the instrument would be direct reading at one value of field only - that for which

$$n_p = 4.25759\, B_o^2 \times 10^{-7} \qquad (7)$$

This method is used in the MNZ1 observatory magnetometer which has provision for setting n_p in the range 100 to 8000 in steps of 100.

Method 2: Used when measurements are required in rapid succession or the readout is to be directly in nanoteslas, e.g. the MNS1 airborne magnetometer and MNS2 general purpose magnetometer.

In this method, the precession frequency is accurately multiplied by a factor N, and the multiplied frequency is gated with a counter by a known number of cycles n_o from a crystal oscillator of frequency F_o Hz. If the counter registers n_c counts, then B_o is given by:

$$B_o = \frac{100}{4.25759} \quad \frac{n_c \; F_o}{n_o \; N} \text{ nansteslas} \qquad (8)$$

---

* Note that the value of γ_p implied in (6) to (9) differs slightly from that in (2). This is because (8) and (9) are applicable to protons in water whereas γ_p is modified by the diamagnetisation of the water molecule.

Note that the field is directly proportional to the counter reading n_c. To make the instrument give a direct and absolute reading for all fields the oscillator frequency should be:

$$F_o = \frac{4.25759}{100} n_o N \quad \text{Hz} \qquad (9)$$

It is convenient to set n_o to be a power of 10 so that decade dividers can be used, and for similar reasons N is set to a multiple of 10. In the MNS1 and MNS2 magnetometers it is desired to perform the measurement in about 1/10 second, so N is set to 200, and n_o to 10^4. Thus F_o is 85.1518 kHz.

ANNOTATED SELECTED BIBLIOGRAPHY

1. Bloch, F., Phys. Rev. 70, 460 (1946). This is the famous paper which introduced the concept of nuclear magnetic induction and predicted the possibility of free precession.

2. Bloch, F., Hansen, W.W. and Packard, M., Ibid. p. 474. This paper describes the first experiments in which forced proton precession was observed.

3. Bloembergen, N., Purcell, E.M., and Pound, R.V., Phys. Rev. 73, 679 (1948). The theory and measurement of nuclear relaxation effects are discussed.

4. Bloembergen, N. and Pound, R.V., Phys. Rev. 95, 8 (1954). A discussion on radiation damping of free precession.

5. Packard, M. and Varian, R., Phys. Rev. 93, 941 (1954). The first paper reporting a proton magnetometer.

6. Waters, G.S., Nature 176, 691 (1955)

7. Waters, G.S. and Phillips, G., Geophysical Prospecting IV, 1-9 (1956) The above two papers report in more detail a magnetometer developed independently in England.

8. Waters, G.S. and Francis, P.D., J. Sci. Instrum. 35, March 1958, p. 88. Contains further details of the English magnetometer.

9. Bender, P.L. and Driscoll, R.L., I.R.E. Transactions on Instrumentation Dec. 1958, p. 176. A method of determining the proton gyromagnetic ratio is presented.

10. Rikitake, T. and Tanaoka, I., Bull. Earthquake Res. Inst. 38, 317 (1960). A proton gradiometer is described.

11. Fiani, G. and Svelto, O., Supplemento al Nuovo Cimento, XXIII, Serie X (1962). Optimization of detector design is considered with a view to maximizing signal to noise ratio.

12. Bullard, E.C., Masom, C.S. and Mudie, J.D., Proc. Camb. Phil. Soc. 60, 287 (1964). The effects of detector ringing on the $\sin^2 \theta$ relationship are discussed.

13. Barrett, D.L., J. Geophys. Res., 73, 16 (1968) p. 5327. A consideration of errors produced by the oscillatory motion of a towed detector.

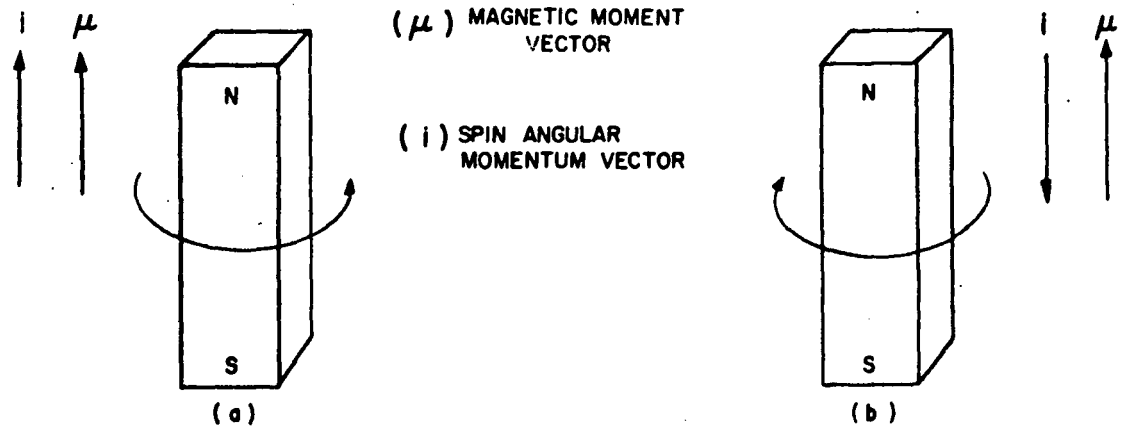

FIG A-1

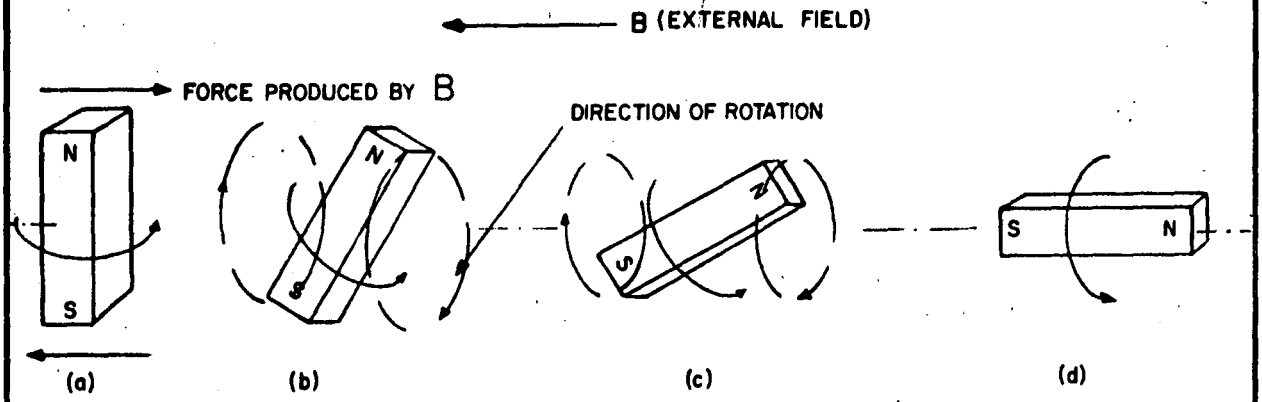

FIG A-2
PRECESSION

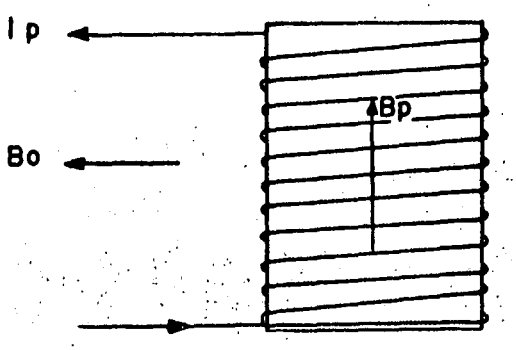

FIG B-1

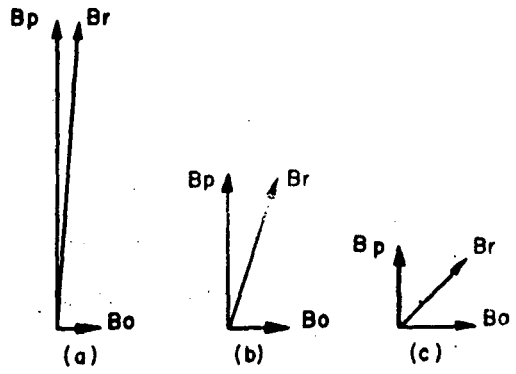

FIG B-2

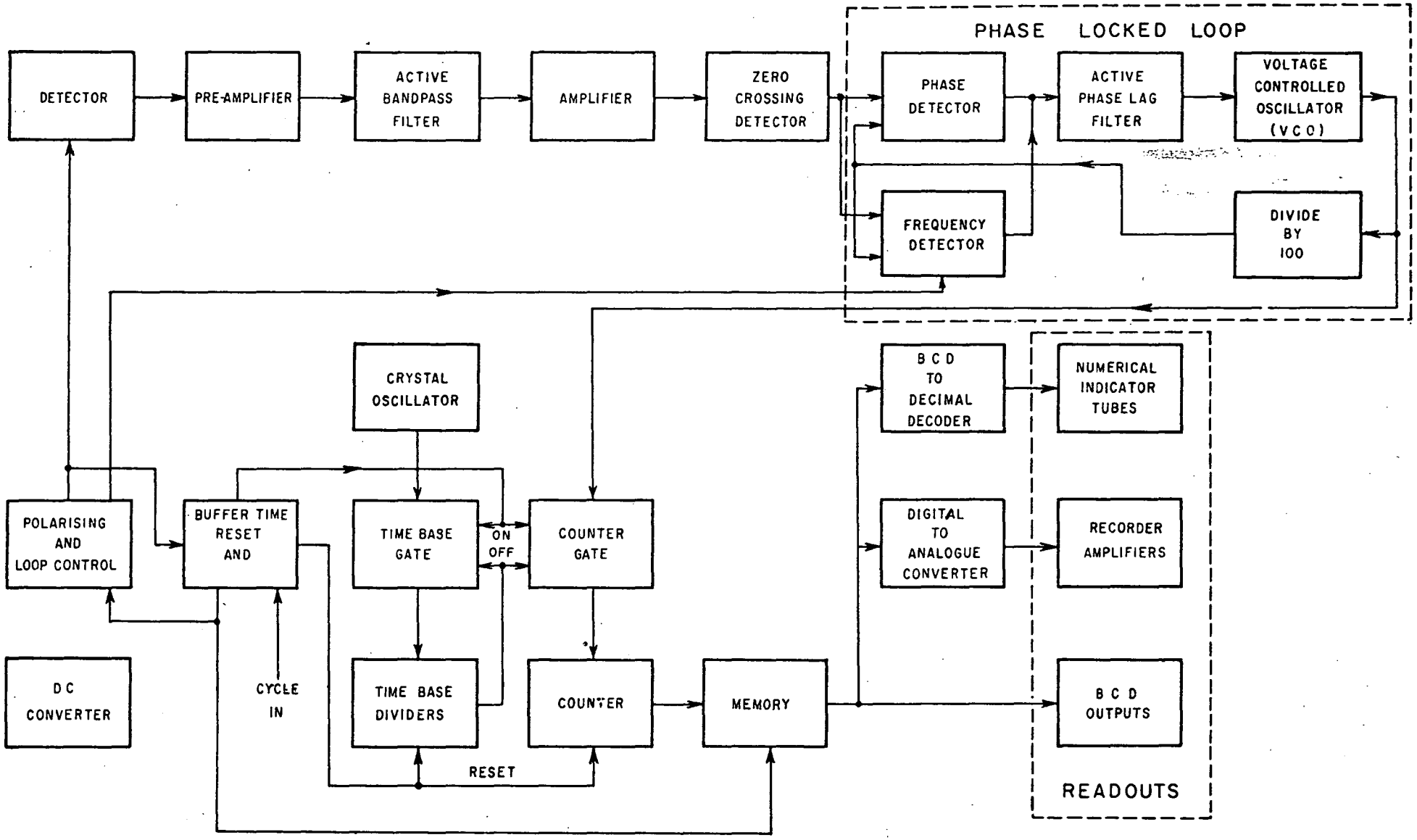

FIGURE 1. MNS 2 SIMPLIFIED BLOCK DIAGRAM

G82/2-124A

TO ACCOMPANY RECORD No. 1970/109